Generic Modeling of a Self-Commutated Multilevel VSC HVDC System for Power System Stability Studies

Christoph Hahn, Matthias Burkhardt,
Anatoli Semerow, Matthias Luther
Chair of Electrical Energy Systems
Friedrich-Alexander-University of Erlangen-Nuremberg
Erlangen, Germany
Christoph.Hahn@fau.de

Olaf Ruhle
Siemens Power Technologies International (PTI)
Siemens AG, Sector Infrastructures and Cities
Erlangen, Germany
Olaf.Ruhle@siemens.com

***Abstract*—This paper provides a generic stability model of a self-commutated multilevel VSC (Voltage Source Converter) HVDC (High Voltage Direct Current) and its appropriate control. At first the approach of modeling depicts the independence of the AC and DC quantities and therefore two separate models – one for the AC and one for the DC side – can be figured out. The AC side model is developed in the dq frame out of the according differential equations. For the DC side no further transformation is required. Regarding the fact of balanced energy terms the two models can be merged.**

The consolidation of both models reveals a comprehensive large signal model of a multilevel based HVDC system which can be used for detailed analyses in power system stability studies. Due to the comparison of the generic stability model with an EMT (Electro-Magnetic Transient) HVDC model the consistence of the dynamic behavior is shown.

Keywords—HVDC Generic Modeling; Modular Multilevel Converter (MMC); VSC Technology; Control Design; HVDC Stability Analyses

I. INTRODUCTION

Due to the turnaround in the German energy policy after Fukushima nuclear disaster the use of HVDC systems has gained a lot of interest as indicated in the German grid development plan [1], where the nuclear power plants – mostly located in the south – will be shut down and the upcoming amount of wind power from the North and East Sea wind parks has to be transported to the load centers in Southern Germany. Due to the advantages of self-commutated multilevel HVDC systems towards line commutated systems – as independence of active and reactive power supply, low harmonic distortion, black start capability, reactive power supply during AC faults, etc. [2] – the German transmission system operators agreed on using this novel technology first introduced from Lesnicar and Marquardt in 2003 [3].

The world's first VSC HVDC transmission was established in Sweden in 1997 in order to connect the Swedish towns of Hellsjön and Grängsberg with a rated power of 3 MW and a length of 10 km [4]. The first VSC HVDC systems were using two and three level technologies which are causing a lot of harmonic noise due to the high switching frequencies in combination with the high voltage level. Trans Bay Cable was the first multilevel VSC HVDC system established in 2010 in San Francisco [5]. The basic scheme of a modular multilevel VSC HVDC system is shown in Figure 1. L_{N1} and L_{N2} are the short circuit reactances of the converter transformer and the connected AC grid which is represented by the three-phase AC sources v_{N1} and v_{N2} respectively. L_{arm} is the converter arm reactance.

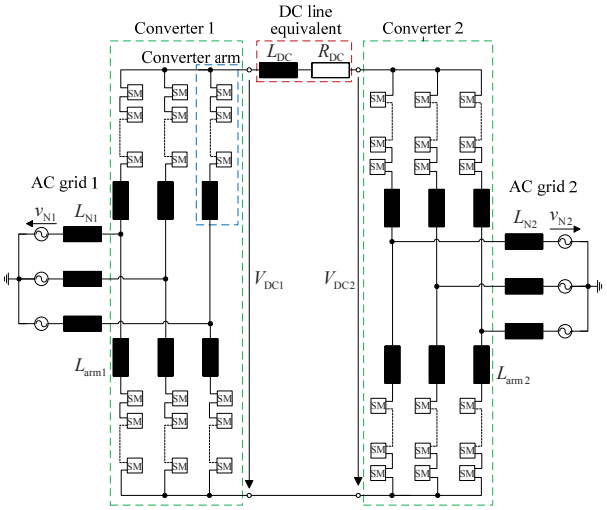

Figure 1: Basic scheme of a modular multilevel VSC HVDC

Currently there are at least two configurations of sub modules (SM) existing which are both illustrated in Figure 2. The big advantage of the full-bridge modules are their capability of handling DC short-circuits [5]. Nevertheless, for multiterminal HVDC systems a DC breaker is required for secure operation [2]. Due to the large amount of series connected sub modules – where each sub module makes its contribution to a voltage shape of very high resolution – the voltage at the connection points of the HVDC is almost perfectly sinusoidal.

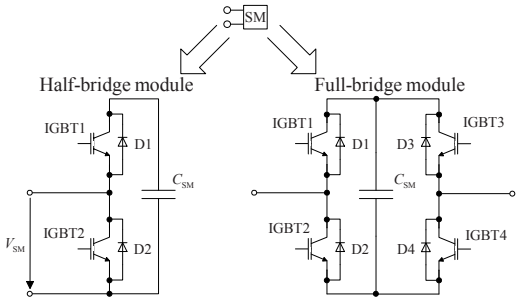

Figure 2: Sub module configuration: half-bridge (left) and full-bridge (right) modules

Some approaches for modeling VSC HVDC systems might for example be found in [6], [7], [8] and also for multiterminal systems in [9] and [10]. These models are often designed for small signal analyses or are too detailed for power system stability studies. Therefore this paper will show the entire development process of a large signal model including the AC side model, the DC side model and the entire control scheme which can be used for power system stability studies.

The developed model will be verified by comparison with an EMT model of a multilevel VSC HVDC system. A start-up process of the HVDC system involving the entire control scheme will be depicted.

II. HVDC Modeling

The first approach of modeling is the replacement of the sub modules (SM) with controllable voltage sources; this is a valid assumption due to their large amount and the resulting high resolution of the AC voltage at the Point of Common Coupling (PCC). In order to gain two independent models, one for the AC and one for the DC side, which are then connected via the terms of energy balancing, the independence of AC and DC side quantities has to be carried out. Therefore a single phase equivalent circuit diagram is depicted in Figure 3.

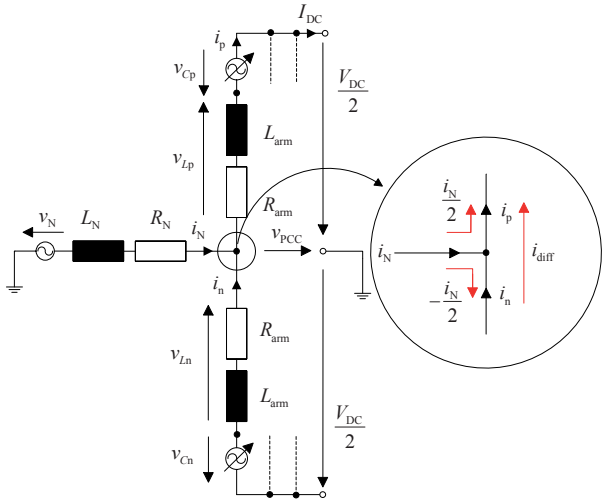

Figure 3: Single phase equivalent circuit diagram with controllable voltage sources

In order to obtain a symmetrical operation the grid current i_N is shared equally at the connection point by the positive and negative converter arm. The circulating current i_{diff} is introduced and therefore the converter arm currents can be defined:

$$i_p = \frac{1}{2} i_N + i_{diff}, \tag{1}$$

$$i_n = -\frac{1}{2} i_N + i_{diff}. \tag{2}$$

After transforming the equations (1) and (2) the grid and circulating current can be stated in dependence of the converter arm currents:

$$i_N = i_p - i_n, \tag{3}$$

$$i_{diff} = \frac{1}{2}\left(i_p + i_n\right). \tag{4}$$

Regarding Figure 3 the following mesh equations can be revealed:

$$v_{PCC} = v_N - R_N i_N - L_N \frac{\mathrm{d}i_N}{\mathrm{d}t}, \tag{5}$$

$$v_{PCC} = \frac{V_{DC}}{2} - v_{Cp} + v_{Lp}, \tag{6}$$

$$v_{PCC} = -\frac{V_{DC}}{2} + v_{Cn} - v_{Ln}. \tag{7}$$

In order to gain a relation between the circulating current i_{diff} and the voltages, equation (7) and (6) were subtracted. Assuming equal impedances and a symmetrical distribution of the currents, the voltage drops across the converter arm impedances can be summarized:

$$V_{DC} = -\left(v_{Ln} + v_{Lp}\right) + v_{Cp} + v_{Cn} = -v_{Lges} + v_{Cp} + v_{Cn}, \tag{8}$$

hence

$$v_{Lges} = \left(v_{Cp} + v_{Cn}\right) - V_{DC}. \tag{9}$$

With the definition of the circulating current and the current-voltage relation at the converter arm impedances the following correlation can be found:

$$\begin{aligned} v_{Lges} &= L_{arm}\left(\frac{\mathrm{d}i_p}{\mathrm{d}t} + \frac{\mathrm{d}i_n}{\mathrm{d}t}\right) + R_{arm}\left(i_p + i_n\right) \\ &= 2L_{arm}\frac{\mathrm{d}i_{diff}}{\mathrm{d}t} + 2R_{arm} i_{diff}. \end{aligned} \tag{10}$$

The appropriate differential equation for the circulating current results out of equation (9) and (10):

$$\frac{\mathrm{d}i_{diff}}{\mathrm{d}t} + \frac{R_{arm}}{L_{arm}} i_{diff} = \frac{1}{2L_{arm}}\left(\left(v_{Cn} + v_{Cp}\right) - V_{DC}\right). \tag{11}$$

Equation (11) shows the controllability of the voltage drop across the converter arm impedance in dependence of the sub module voltages v_{Cn} and v_{Cp}. In order to gain an expression for the grid current i_N the sum of the equations (6) and (7) has to be stated:

$$2v_{PCC} = v_{Cn} - v_{Cp} + v_{Lp} - v_{Ln}. \tag{12}$$

Regarding the current-voltage relation at the converter arm impedance and the definition of the grid current i_N according to equation (3), the following expression can be found:

$$\frac{\mathrm{d}i_N}{\mathrm{d}t} + \frac{R_{arm}}{L_{arm}} i_N = \frac{1}{L_{arm}}\left(2v_{PCC} + \left(v_{Cp} - v_{Cn}\right)\right). \tag{13}$$

Comparing the equations (11) and (13) yields in the fact that the circulating current i_{diff} can be controlled by the sum of v_{Cn} and v_{Cp} and the grid current i_{N} can be controlled by the difference of both voltages. As the sum and the difference of both voltages are linearly independent, both quantities can be controlled independently.

A. AC side Modell

Inserting equation (5) in (13) yields in equation (14). By using this approach the converter arm quantities can be transformed in phase quantities as illustrated in Figure 4.

$$\left(L_{\text{N}}+\frac{L_{\text{arm}}}{2}\right)\frac{\mathrm{d}i_{\text{N}}}{\mathrm{d}t}+\left(R_{\text{N}}+\frac{R_{\text{arm}}}{2}\right)i_{\text{N}}=v_{\text{N}}-\frac{v_{\text{Cn}}-v_{\text{Cp}}}{2} \tag{14}$$

As the electrical potential $(v_{\text{Cn}}-v_{\text{Cp}})/2$ plays an important role for the control of the converter, it will be named e_{PCC} hereinafter. Applying this procedure according to [6] and [11] to all three phases the equivalent circuit diagram can be derived out of equation (14) and is shown in Figure 4.

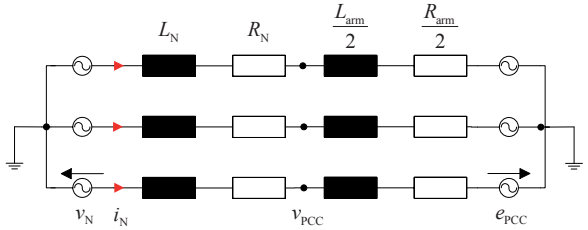

Figure 4: AC equivalent circuit diagram of the MMC

As equation (14) shows the voltage e_{PCC} is only dependent of the grid voltage and current and therefore independent of the DC side.

In order to obtain a simpler mathematical model in the Laplace domain the Park-transformation is applied. For a symmetrical three phase AC system the Park-transformation provides zero-frequency quantities and therefore control design is much easier too. Applying the Park transformation on equation (14) yields:

$$\begin{pmatrix}v_{\text{N\_d}}\\v_{\text{N\_q}}\\v_{\text{N\_0}}\end{pmatrix}=\underbrace{\mathbf{T}_{\text{abc/dq0}}\mathbf{L}\mathbf{T}^{-1}_{\text{abc/dq0}}}_{\mathbf{L}_{\text{dq0}}}\frac{\mathrm{d}}{\mathrm{d}t}\begin{pmatrix}i_{\text{N\_d}}\\i_{\text{N\_q}}\\i_{\text{N\_0}}\end{pmatrix}+ \underbrace{\left\{\mathbf{T}_{\text{abc/dq0}}\mathbf{R}\mathbf{T}^{-1}_{\text{abc/dq0}}+\mathbf{T}_{\text{abc/dq0}}\mathbf{L}\frac{\mathrm{d}}{\mathrm{d}t}\mathbf{T}^{-1}_{\text{abc/dq0}}\right\}}_{\mathbf{R}_{\text{dq0}}}\begin{pmatrix}i_{\text{N\_d}}\\i_{\text{N\_q}}\\i_{\text{N\_0}}\end{pmatrix}+\begin{pmatrix}e_{\text{PCC\_d}}\\e_{\text{PCC\_q}}\\e_{\text{PCC\_0}}\end{pmatrix}, \tag{15}$$

where $\mathbf{R}=\text{diag}\left\{R_{\text{N}}+\frac{R_{\text{arm}}}{2}\right\}$, $\mathbf{L}=\text{diag}\left\{L_{\text{N}}+\frac{L_{\text{arm}}}{2}\right\}$ and $\mathbf{T}_{\text{abc/dq0}}$ is the transformation matrix into the dq frame and $\mathbf{T}^{-1}_{\text{abc/dq0}}$ its inverse respectively. After some calculations the system of equations in the dq frame reveals under neglection of the zero component due to the assumption of a symmetrical system, where $R=R_{\text{N}}+\frac{R_{\text{arm}}}{2}$ and $L=L_{\text{N}}+\frac{L_{\text{arm}}}{2}$:

$$\begin{pmatrix}v_{\text{N\_d}}\\v_{\text{N\_q}}\end{pmatrix}-\begin{pmatrix}e_{\text{PCC\_d}}\\e_{\text{PCC\_q}}\end{pmatrix}=\underbrace{\begin{pmatrix}L&0\\0&L\end{pmatrix}}_{\mathbf{L}_{\text{dq}}}\frac{\mathrm{d}}{\mathrm{d}t}\begin{pmatrix}i_{\text{N\_d}}\\i_{\text{N\_q}}\end{pmatrix}+\underbrace{\begin{pmatrix}R&-\omega L\\\omega L&R\end{pmatrix}}_{\mathbf{R}_{\text{dq}}}\begin{pmatrix}i_{\text{N\_d}}\\i_{\text{N\_q}}\end{pmatrix}. \tag{16}$$

This system of equations can be transformed into the Laplace domain and solved for the currents which are the output variables of the system; hence the equations (17) and (18) can be stated.

$$i_{\text{N\_d}}=\left[v_{\text{N\_d}}-e_{\text{PCC\_d}}+\omega L i_{\text{N\_q}}\right]\frac{1}{R}\cdot\frac{1}{1+\frac{L}{R}\text{s}} \tag{17}$$

$$i_{\text{N\_q}}=\left[v_{\text{N\_q}}-e_{\text{PCC\_q}}-\omega L i_{\text{N\_d}}\right]\frac{1}{R}\cdot\frac{1}{1+\frac{L}{R}\text{s}} \tag{18}$$

Based on the equations (17) and (18) the block diagram can be designed as depicted in Figure 5.

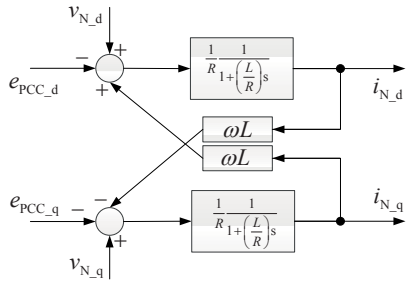

Figure 5: Block diagram of the AC side model

B. DC side Modell

Analogously to the approach for the AC side a dynamic model for the DC side can be obtained from equation (11). As can be easily seen i_{diff} is only dependent on internal converter quantities. Hence the voltage v_{diff} can be introduced which describes the dynamics of the DC side of the converter:

$$v_{\text{diff}}=L_{\text{arm}}\frac{\mathrm{d}i_{\text{diff}}}{\mathrm{d}t}+R_{\text{arm}}i_{\text{diff}}=\frac{v_{\text{Cn}}+v_{\text{Cp}}}{2}-\frac{V_{\text{DC}}}{2}. \tag{19}$$

Therefore an equivalent circuit diagram can be designed as depicted in Figure 6.

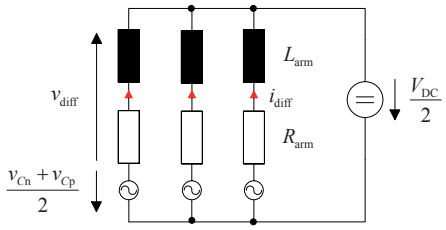

Figure 6: DC equivalent circuit diagram of the MMC

In a steady state condition, where no equalization currents are assumed between the phase modules and therefore the converter operates in an energy balanced mode, the following simplifications can be stated:

$$\sum_{i=\text{a,b,c}}i_{\text{diff\_}i}=\frac{1}{2}\sum_{i=\text{a,b,c}}\left(i_{\text{p\_}i}+i_{\text{n\_}i}\right)=I_{\text{DC}}, \tag{20}$$

$$v_{\text{Cp}}+v_{\text{Cn}}-2L_{\text{arm}}\frac{\mathrm{d}i_{\text{diff}}}{\mathrm{d}t}-2R_{\text{arm}}i_{\text{diff}}=V_{\text{DC}}\ \text{(acc. to Fig. 3).} \tag{21}$$

The equivalent DC circuit diagram of the HVDC system out of Figure 1 can be illustrated as shown in Figure 7.

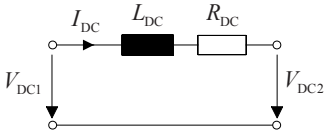

Figure 7: DC circuit of the multilevel VSC HVDC

The differential equation describing the voltage and current relations of the DC circuit is the following:

$$V_{DC1} - V_{DC2} = RI_{DC} + L_{DC}\frac{dI_{DC}}{dt}, \tag{22}$$

which can be transferred into the Laplace domain and separated to the DC current:

$$I_{DC} = \left(V_{DC1} - V_{DC2}\right)\frac{1}{R_{DC}}\frac{1}{1+s\frac{L_{DC}}{R_{DC}}}. \tag{23}$$

Therefore the block diagram of the DC circuit can be depicted according to Figure 8.

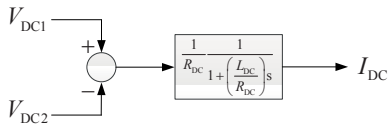

Figure 8: Block diagram of the DC circuit

Having a closer look to the structure of the MMC reveals the occurrence of many distributed capacitors belonging to the sub modules (Figure 2). The first approach of modeling was the replacement of the sub modules with controllable voltage sources. This is a valid assumption as long as the voltage sources are operated in an energy balanced mode. Nevertheless the dynamics of the distributed capacitors is neglected. For that reason an additional capacitor can be inserted in the DC circuit which comprises the dynamic behavior of the entire capacitors belonging to the sub modules:

$$C = C_{DC} + \frac{C_{SM}}{n_{mod}} \cdot 6. \tag{24}$$

C_{SM} is the capacity of one sub module (Figure 2). n_{mod} is the number of capacitors belonging to one phase (series connection of two converter arms) and for two converters there are six phases in parallel. C_{DC} might be an additional capacity of the DC circuit which can be taken into account. The equivalent DC circuit diagram considering the dynamics of the distributed sub module capacitors is depicted in Figure 9.

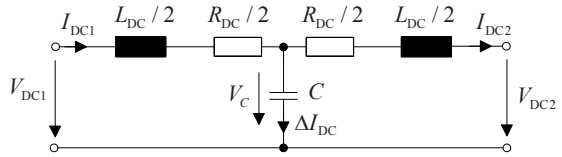

Figure 9: Equivalent DC circuit of the multilevel VSC HVDC considering the distributed sub module capacitors

Writing down the differential equations for this circuit and transferring the set of equations into the Laplace domain reveals in a block diagram as depicted in Figure 10.

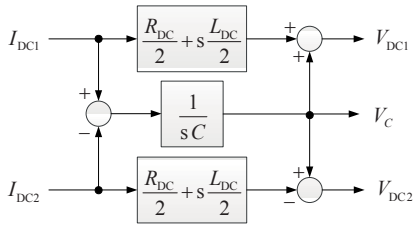

Figure 10: Block diagram of the DC circuit considering the distributed sub module capacitors

C. MMC HVDC Model

In order to combine both models the fact of balanced energy terms has to be kept in mind. As the outlined voltage sources are a series connection of capacitors in reality, they only have a limited energy storage capacity in opposite to ideal voltage sources. By this means, the power which is obtained from AC grid 1 (Figure 1) has to be transferred to AC grid 2 via the DC circuit. This fact can be used in order to combine the models via the power equations for the DC and AC side in dq components respectively, where $v_{N\_q} = 0$ due to the definition of the rotating coordinate system:

$$P = \frac{3}{2} v_{N\_d}\, i_{N\_d} = V_{DC} I_{DC} \tag{25}$$

Now the block diagram of the model of the MMC HVDC system can be presented in Figure 11 considering a DC circuit as illustrated in Figure 7 or Figure 8 respectively.

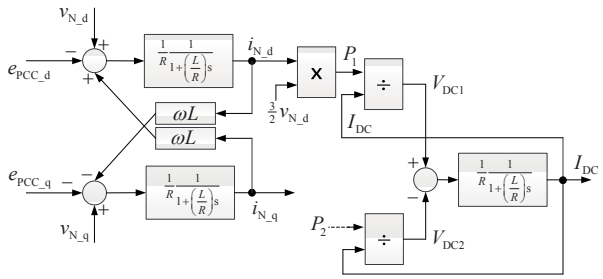

Figure 11: Block diagram of the model of the multilevel VSC HVDC

III. Control

As the AC part of the multilevel VSC HVDC system was built up in the dq frame, the control system will be built up in the dq frame too.

A cascaded control system with an inner current control and an outer power/voltage control can be applied to the system [6]. Using this control strategy makes the application of a decoupling filter in the inner current controller in order to eliminate the coupling terms between the dq currents and voltages (Figure 5) possible.

Only one converter has the ability of controlling the active power and the other converter has to deliver the remaining power from the converter which handles the active power control. Therefore the task of the second converter is the DC voltage control. Both converters are able to control

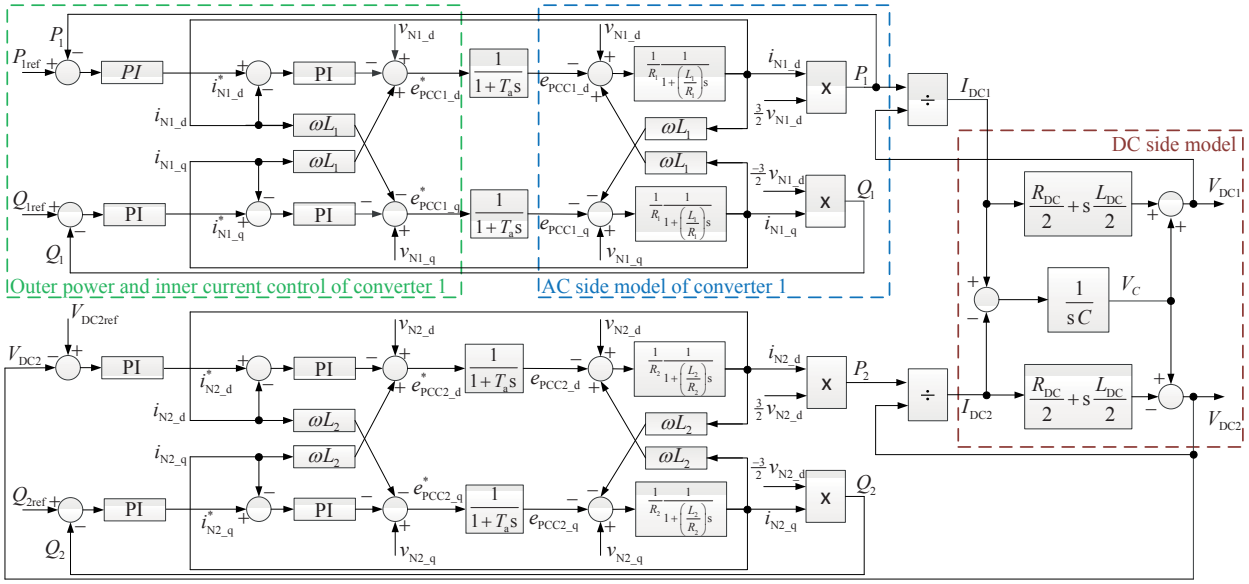

Figure 12: Block diagram of the entire multilevel VSC HVDC system with its apropriate control

their reactive power independently. The reactive power in dq components can be calculated as follows:

$$Q = -\frac{3}{2} v_{N\_d}\, i_{N\_q} \tag{26}$$

The block diagram of the entire multilevel VSC HVDC system with its appropriate cascaded control systems is illustrated in Figure 12 considering a DC circuit as depicted in Figure 9 or Figure 10 respectively. T_a might represent the time lag due to the discretization of the control signal for the series connection of the sub modules.

IV. Results and Comparison with an EMT Modell

The developed model and its appropriate control system as described in the previous chapters were implemented in the mathematical standard software MATLAB/Simulink® and PSS®NETOMAC. In order to verify the behavior of the developed mathematical stability model, an EMT model using a setup as depicted in Figure 1 – where the series connection of sub modules were replaced with controlled voltage sources – was built up in MATLAB/Simulink® using the SimPowerSystems® Toolbox.

In order to compare both models a startup process of the HVDC system was performed as depicted in Figure 13. The DC circuit configuration was chosen with regard to Figure 7 or Figure 8 respectively. The set-points for the active and reactive power were ramped up with a time constant of one second as it was done for the DC voltage set-point. The DC current rises up very fast as the second converter controls the voltage and has to take over the remaining active power of converter 1. After $t = 2$ sec the set-points of power and voltage were changed to 20 % of its original set-point and ramped down. After four seconds the new operating point is reached and the model operates in a new steady state condition. Both models are matching in a broad range as Figure 13 shows. Simulation parameters were chosen according to Table I and can be obtained e.g. from [6], [12], [13] and [14].

Figure 14 shows a startup process of the HVDC system with a subsequent power reversal and a DC circuit configuration taking the dynamics of the distributed sub module capacitors into account according to Figure 9 or Figure 10 respectively. The model was connected to two AC grids according to Figure 1 using so called Three Phase Dynamic Load blocks (VAR-*P*/*Q*). Additionally the transformer tap changers were modelled as described in [12] in order to control the voltage at the connection point.

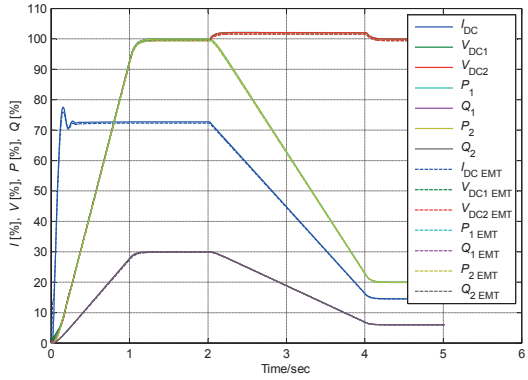

Figure 13: Comparison of the EMT and stability model during a startup process

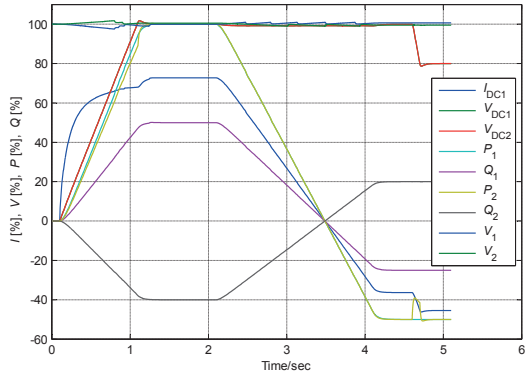

Figure 14: Startup process and subsequent power reversal of the HVDC model

During the startup process the AC voltage drops due to the infeed of reactive power which was set to this specific set-point but is not necessarily like this. Thereupon the tap changer control reacts and steps up in order to hold the desired AC

voltage. It can be seen that there is a difference between P_1 and P_2 during the startup process. The area lying in between the curves is the amount of energy which charges the sub module capacitors during the startup process. After $t = 2$ sec a power reversal to a set-point of - 50 % of the original set-point was performed. Due to the change of reactive power infeed the tap changer has to switch several times. After $t = 4.5$ sec the set-point of the DC voltage was changed to 80 % of its original set-point. During this process P_2 shortly drops due to the discharge of the sub module capacitors as they ensure the constancy of P_1.

Table I: HVDC parameters for simulation

$f_{N1} = f_{N2}$	50 Hz	P_{ref}	1000 MW
$V_{N1} = V_{N2}$	380 kV	V_{DCref}	640 kV
$R_{N1} = R_{N2}$	0.824 Ω	K_{p_i}	0.1
$L_{N1} = L_{N2}$	26.8 mH	T_{N_i}	0.003 sec
R_{arm}	0.47 Ω	$K_{p\_P\_Q}$	0.1
L_{arm}	15 mH	$T_{N\_P\_Q}$	0.006 sec
R_{DC}	0.1 Ω	L_{DC}	85 mH
C_{SM}	4.5 mF	n_{SM}	216

V. Conclusion

In this paper the development process of a large signal model of a multilevel VSC HVDC system was shown. At the beginning the independence of the AC and DC side quantities was shown and therefore two different models – one for the AC and one for the DC side – were developed. Furthermore the distributed capacitors of the sub modules were taken into consideration for the model. Both models were connected via the terms of energy balancing and the appropriate control system was added.

The developed mathematical stability model was then compared with an EMT model using controlled voltage sources and a high correlation between the models could be figured out. A startup process of the HVDC system with a subsequent power reversal was also shown.

The model was implemented in MATLAB/Simulink® and PSS®NETOMAC and can be used for detailed power system stability studies as it comprises a detailed large signal model with its entire control scheme.

VI. References

[1] O. Feix, R. Obermann, M. Strecker, and A. Brötel, *German grid development plan 2013, (Netzentwicklungsplan Strom 2013)*. Berlin, Germany: The German Transmission System Operators, 2013.

[2] J. Dorn, H. Huang, and D. Retzmann, "Novel Voltage-Sourced Converters for HVDC and FACTS Applications," in *CIGRE Conference*, pp. n/s. Osaka, Japan. 28-31 Oct. 2007.

[3] A. Lesnicar and R. Marquardt, "An innovative modular multilevel converter topology suitable for a wide power range," in *2003 IEEE Bologna Power Tech*, pp. 272–277. Bologna, Italy. June 23-26, 2003.

[4] D. Oeding and B. R. Oswald, *Electric Power Stations and Grids (Elektrische Kraftwerke und Netze),* 7th ed. Heidelberg: Springer, 2011 (in German).

[5] J. Dorn, H. Gambach, J. Strauss, T. Westerweller, and J. Alligan, "Trans Bay Cable – A Breakthrough of VSC Multilevel Converters in HVDC Transmission," in *CIGRE Colloquium*, pp. n/s. San Francisco, USA. 2012.

[6] S. Liu, Z. Xu, W. Hua, G. Tang, and Y. Xue, "Electromechanical Transient Modeling of Modular Multilevel Converter Based Multi-Terminal HVDC Systems," *IEEE Trans. Power Syst,* vol. 29, no. 1, pp. 72–83, 2014.

[7] M. Guan and Z. Xu, "Modeling and Control of a Modular Multilevel Converter-Based HVDC System Under Unbalanced Grid Conditions," *IEEE Trans. Power Electron,* vol. 27, no. 12, pp. 4858–4867, 2012.

[8] J. Peralta, H. Saad, and S. Dennetiere, "Dynamic performance of average-value models for multi-terminal VSC-HVDC systems," in *2012 IEEE Power & Energy Society General Meeting. New Energy Horizons - Opportunities and Challenges*, pp. 1–8. San Diego, CA. 22–26 July 2012.

[9] J. Beerten and R. Belmans, "Modeling and Control of Multi-Terminal VSC HVDC Systems," *Selected papers from Deep Sea Offshore Wind R&D Conference, Trondheim, Norway, 19-20 January 2012*, vol. 24, no. 0, pp. 123–130, 2012.

[10] T. M. Haileselassie, M. Molinas, and T. Undeland, "Multi-Terminal VSC-HVDC System for Integration of Offshore Wind Farms and Green Electrification of Platforms in the North Sea," in *NORPIE/2008, Nordic Workshop on Power and Industrial Electronics*, pp. n/s. Helsinki, Finland. 9-11 June 2008.

[11] M. Zhang, L. Huang, W. Yao, and Z. Lu, "Circulating Harmonic Current Elimination of a CPS-PWM-Based Modular Multilevel Converter With a Plug-In Repetitive Controller," *IEEE Trans. Power Electron,* vol. 29, no. 4, pp. 2083–2097, 2014.

[12] C. Hahn, A. Semerow, M. Luther, and O. Ruhle, "Generic Modeling of a Line Commutated HVDC System for Power System Stability Studies," in *2014 IEEE PES Transmission & Distribution Conference and Exposition*, pp. n/s. Chicago, USA. April 2014.

[13] P. L. Francos, S. S. Verdugo, H. F. Alvarez, S. Guyomarch, and J. Loncle, "INELFE — Europe's first integrated onshore HVDC interconnection," in *2012 IEEE Power & Energy Society General Meeting. New Energy Horizons - Opportunities and Challenges*, pp. 1–8. San Diego, CA, USA. July 2012.

[14] P. Münch, *Conception and Design of integrated Controls for Modular Multilevel Converter (Konzeption und Entwurf integrierter Regelungen für modulare Multilevel-Umrichter)*. Berlin: Logos-Verl, 2011 (in German).

Biographies

Christoph Hahn received his Dipl.-Ing. degree from the University of Erlangen-Nuremberg, Germany, in 2011. Currently he is a Ph.D. student and research associate at the Chair of Electrical Energy Systems at the University of Erlangen-Nuremberg, Germany. His research interests lie in the field of HVDC modeling and control.

Matthias Burkhardt received his B.Sc. degree from the University of Erlangen-Nuremberg, Germany, in 2013. Currently he is a M.Sc. student at the Chair of Electrical Energy Systems at the University of Erlangen-Nuremberg, Germany.

Anatoli Semerow received his B.Eng. degree in 2009 from the University of Applied Sciences of Hannover, Germany, and his M.Sc. degree in 2011 from Technical University of Clausthal, Germany. Since 2011 he has been working as a research associate at the University of Erlangen-Nuremberg, Germany. His research interests are related to Power System Stability and Control.

Matthias Luther studied electrical engineering and received his Ph.D. at the Technical University of Brunswig, Germany in 1992. From 1993 he held different functions and management positions in the electricity industry at PreussenElektra, E.ON Netz and TenneT TSO. Since 2011 he is professor and holds the Chair of Electrical Energy Systems at the University of Erlangen-Nuremberg, Germany.

Olaf Ruhle received his Dipl.-Ing. and his Ph.D. degree in electrical engineering from the Technical University of Berlin in 1990 and 1994 respectively. Since 1993 he is a member of Power Transmission and Distribution Group and the system planning department at Siemens in Erlangen, Germany. He is responsible for the program system PSS®NETOMAC support, sale and training worldwide. He is visiting professor at several universities.